Chapter 19
Joint Acquisition and Processing of Seismic Reflections and Surface Waves in a Sensitive Clay Deposit in the Outaouais Region (Québec), Canada

Gabriel Fabien-Ouellet, Richard Fortier, and Bernard Giroux

Abstract The joint acquisition and processing of vertically polarized shear (*SV*) wave seismic reflections and surface waves during a seismic survey were carried out in Buckingham (Québec), near Ottawa, Canada, to characterize a thick (20–40 m) sensitive clay deposit. At the study site, the outcropping clay unit overlays a 20–50 m thick layer of sand and gravel and the bedrock depth reaches more than 90 m along the survey line. The seismic reflection survey using common-mid-point (CMP) inversion of *SV*-wave reflections allowed the localization of the clay-sand and sand-bedrock interfaces as well as the measurement of *SV*-wave velocities down to the bedrock contact. Velocity variations at depths less than 10 m could not be assessed due to the early reflections hidden by seismic arrivals such as surface waves. However, multi-channel analysis of surface waves (MASW) provided the variations in *S*-wave velocity from the surface down to a depth of 12 m at each CMP location. The joint acquisition and processing of *SV* reflections and Rayleigh waves provided a more complete and accurate 2D *SV* velocity model than both methods taken separately. To test the accuracy of the proposed approach, a multi-offset seismic piezocone penetration test (SCPTu) was performed along the survey line from the surface down to a depth of 25 m. The vertical variations in seismic velocities in sensitive clay as inferred from the *SV* seismic reflection survey and MASW are comparable to the SCPTu *S*-wave profile.

Keywords Seismic reflection survey • Vertically polarized shear waves • Multi-channel analysis of surface waves (MASW) • Vertical seismic profiling (VSP) • Multi-offset seismic piezocone penetration test (SCPTu) • Sensitive clay

G. Fabien-Ouellet (✉) • R. Fortier
Département de géologie et de génie géologique, Université Laval,
Québec City, QC, Canada
e-mail: gabriel.fabien-ouellet.1@ulaval.ca

B. Giroux
INRS-ETE, Québec City, QC, Canada

J.-S. L'Heureux et al. (eds.), *Landslides in Sensitive Clays: From Geosciences to Risk Management*, Advances in Natural and Technological Hazards Research 36,
DOI 10.1007/978-94-007-7079-9_19,

19.1 Introduction

Shear-wave velocity is a fundamental parameter for assessing the dynamic properties of soils in areas prone to earthquakes and landslides. This led the National Building Code of Canada to include shear-wave velocity at a 30-m depth (Vs_{30}) in the definition of the soil classification categories (Finn and Wightman 2003). Several methods are available for the measurement of Vs_{30}; the most common being vertical seismic profiling (VSP) and multi-channel analysis of surface waves (MASW). Both methods have serious drawbacks for very thick (>50 m) and soft soils, as deep drilling, needed for VSP, becomes cost prohibitive, and the depth of investigation of the active MASW method is somewhat limited. Recently, seismic reflection surveys using vertically polarized shear (*SV*) waves have been used in conjunction with the landstreamer technology to efficiently investigate thick clay deposits (Pugin et al. 2009). Heavy and expensive vibratory sources were used in these surveys to generate *SV*-waves. An alternative approach to evaluate Vs_{30} is proposed in this paper using the joint processing of *SV* reflections and Rayleigh waves acquired during a typical seismic reflection survey using a straightforward hammer impact on a steel plate as a seismic source. The MASW method is first used to process Rayleigh waves and obtain a velocity model for the first meters of soil. Those results are then integrated in the semblance analysis of the *SV* reflection data to produce a complete 2D velocity model of the overburden as well as a stacked seismic reflection profile. A case study on this alternative approach is presented for investigating a thick (>30 m) sensitive clay deposit in the Outaouais region (Québec), Canada. For this case study, the proposed approach was effectively used to assess a 2D shear-wave velocity model along a 1 km long survey line from the surface down to depths as great as 90 m. The velocity model is finally compared with the results of a multi-offset seismic piezocone penetration test (SCPTu) carried out at one location along the survey line to test its accuracy in a blind test.

19.2 Study Site

The study site is located in the Outaouais region (Québec), Canada, close to the city of Ottawa. This region is at high risk of landslides due to thick sensitive clay deposits and seismic activity (Aylsworth et al. 2000). Extensive studies were carried out in this region to assess these risks (Motazedian and Hunter 2008). Several seismic methods were used in these studies, in particular downhole seismic, MASW, seismic reflection and refraction, and spectral ratio methods.

The Quaternary geology of the Outaouais region consists of a thin veneer of till overlain with glaciofluvial sediments mainly composed of sands and gravels. This sequence is covered by a marine unit deposited by the Champlain Sea around 11,400 years. BP and composed of sensitive clay. The study area and the seismic line location are shown in Fig. 19.1. According to the logs of nearby wells, the thickness of the clay deposit ranges between 10 and 35 m while the thickness of the

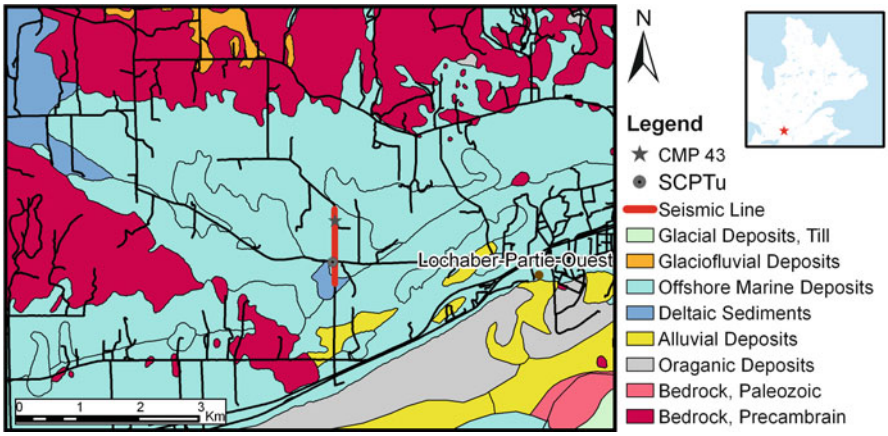

Fig. 19.1 Map of Quaternary deposits (Modified from Bélanger et al. 1997). The locations of the seismic reflection survey line, CMP gather no. 43 and SCPTu are identified by a thick *red line*, a *grey star*, and a *grey circle* respectively

glaciofluvial unit varies between 20 and 60 m. There is no till in contact with the bedrock. The depth to bedrock ranges from 40 to 90 m along the survey line. Due to the outcropping clay unit and the thick overburden, the study site is suitable for testing the proposed approach.

19.3 Combined MASW-SV Seismic Reflection Survey

19.3.1 Field Data Acquisition

The seismic reflection survey was designed primarily for the acquisition of *SV*-wave reflections. Parameters were chosen according to the walk-away method proposed by Steeples and Miller (1998). The survey parameters are given in Table 19.1. A straightforward hammer impact on a steel plate lying on the ground surface was used as a seismic source. The survey was carried out on the shoulder of a dirt road. Despite difficult source and geophone coupling on this kind of surface, a good signal was obtained for Rayleigh waves, *SV*- and *P*-wave reflections.

Although a single 24-channel Geode was used, 96 traces per shot position were acquired by revisiting each shot position four times as the spread cable was moved forward along the line. This configuration was required to meet the constraints of geophone spacing and spread length. Indeed, small geophone spacing is required for *SV* reflection surveys to avoid aliasing of reflection hyperbolas while long spread cable is needed for a better coverage of *P*-wave reflections. Moreover, this configuration meets the guidelines for the MASW method when the depth to bedrock is in excess of 50 m. In such case, according to Park et al. (2002), the maximum offset

Table 19.1 Acquisition parameters for the combined MASW-seismic reflection survey

Source	Stack	Geophone frequency	Source spacing	Geophone spacing	Minimum offset	Shot point fold
8 kg hammer	2	30 Hz	3 m	0.75 m	0.75–6.75 m	96

should be around 100 m and the geophone spacing around 1 m. This is the case for the present survey. However, they also recommend the use of 4.5 Hz geophones, while 30 Hz geophones were used instead. Although lower frequencies are preferable for MASW, the surface wave analysis performed on this dataset was done without too much loss of information, as shown in the next section.

19.3.2 MASW Processing

MASW processing was applied as described in Park et al. (1998). After specifying the geometry for each shot file, the traces were sorted by their common-middle-point (CMP) with a binning of 6 m, resulting in a 192 fold. With such a high fold, there is no loss using CMPs instead of shot gathers. These steps were performed with the help of CREWES MATLAB package (Margrave 2003) and in-house MATLAB codes. All the remaining processing steps were carried out using SeisImager/SW software package.

The fundamental mode of each CMP was handpicked and smoothed using a median filter. An initial model containing 15 layers ranging from the surface down to a depth of 12 m was assigned to each dispersion curve. They were inverted individually using the algorithm described in Xia et al. (1999), keeping only the layer thickness fixed. The resulting models were linearly interpolated to obtain a 2D velocity profile.

The dispersion curve for the CMP gather no. 43 is shown in Fig. 19.2b. The first mode appears clearly between 3 and 15 Hz and higher modes are also present. The dispersion curves are very smooth because of the high CMP fold. The estimated picking error is also shown in Fig. 19.2b and its effect on the inverted model is shown in Fig. 19.2c. The mean variation between the inverted models due to picking errors is 4 %, slightly higher than the picking error itself (3 %).

Although the response of 30 Hz geophones is not flat below 30 Hz, it did not hinder too much the MASW processing. First, each frequency is normalized on the dispersion curves, so amplitude attenuation is not a concern, as long as the signal can be detected. Moreover, spurious frequencies generated by calculation artefacts would not generate the continuous and sharp dispersion patterns seen in Fig. 19.2b. All those facts support the claim that frequencies as low as 3 Hz were effectively detected on the dispersion curves. The use of 4.5 Hz geophones could help the detection of lower frequencies. However, it is doubtful that a hammer can produce frequencies much lower than 2 Hz, and the gain in penetration depth would not be enough to reach the bedrock.

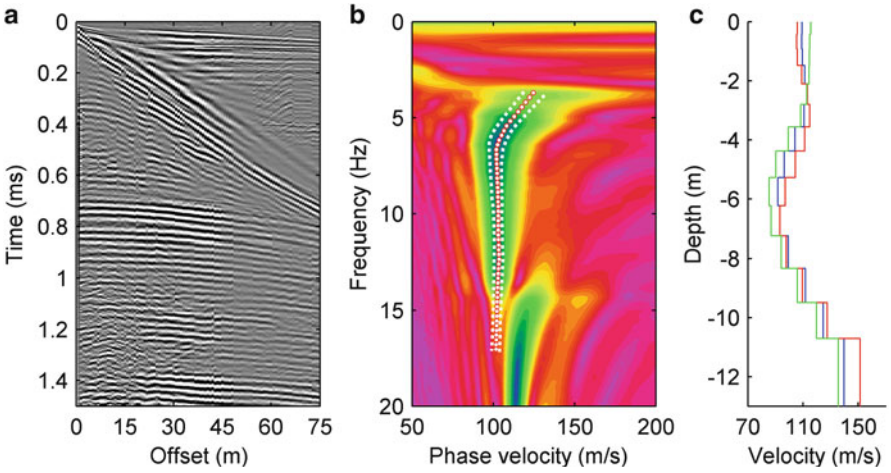

Fig. 19.2 CMP gather no. 43 (**a**), its dispersion curve (**b**) with the selected first mode (*orange circles*) and the picking error (*dotted white lines*). The inverted model is shown in *blue* in (**c**). The maximum and minimum models due to picking error are shown in *red* and *green* respectively

Table 19.2 CMP processing of *SV* seismic reflections

Processing steps	Comments
1. Geometry	Position and elevation of the shots and geophones
2. Bad trace removal	Automatic filter based on S/N ratio
3. Surface wave filter	Based on the dispersion of surface waves
4. Scaling	AGC with a 200 ms window
5. CMP binning	Bin length: 6 m
6. MASW model V_{RMS} conversion	Included in step 7
7. Semblance analysis	Each CMP was processed
8. Velocity conversion	V_{RMS} conversion to interval velocity

19.3.3 SV Seismic Reflection Combined Processing

The CMP data processing flow for *SV* seismic reflections is summarized in Table 19.2. Two programs were used: CREWES MATLAB package for steps 1, 2, 3, 6 and 8 and GEDCO Vista for the remaining steps. The surface wave filter in step 3 is based on the dispersion of surface waves and more details on its performance will be published later. The processing flow was designed to produce a 2D *SV* velocity section; so post velocity analysis steps leading to a stacked section are not given and detailed herein.

The semblance analysis of the CMP gather no. 43 is given in Fig. 19.3. The quality of the semblance panel is judged very good for this example since each reflection has a quite isolated semblance peak. *SV* reflections can be observed from 150 ms to the end of the record. The bedrock reflection is at about 750 ms. All reflections at later times are multiples and are not included in the velocity analysis. This is

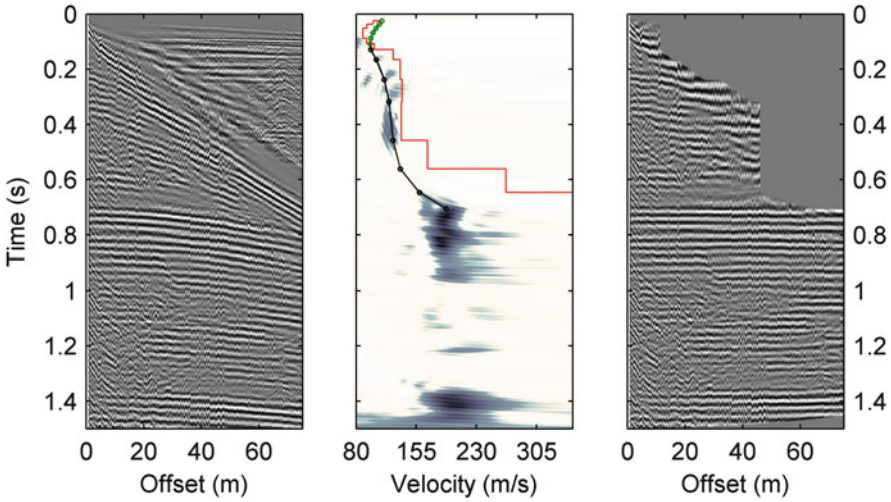

Fig. 19.3 CMP gather no. 43 (*left*), its semblance analysis (*middle*) and the NMO corrected gather (*right*) with a 100 % stretch mute. Selected RMS velocities are shown in *black* and the interval velocities are shown in *red*. The *green circles* are the velocities derived from the MASW method

supported by the velocity inversion after 750 ms on the semblance panel, which is unrealistic for reflections below the bedrock. *P*-wave reflections are located at the top-right of the gather and are clearly separated from *SV*-wave reflections. The processing of both *SV*- and *P*-waves reflections on the CMP gathers can therefore be performed.

Because there is no distinguishable reflection before 150 ms, earlier velocities in Fig. 19.3 are derived from the MASW results as mentioned in step 6 of the processing flow (Table 19.2). In the present case, MASW can give velocities from the surface down to a depth of about 12 m. This limited depth of investigation is caused by the very low seismic velocities in sensitive clay, which yield a small wavelength even at low frequencies. *SV* reflections are distinguishable from about 150 ms or at a depth of about 10 m for an average velocity of 130 m/s. Therefore, both methods are complementary and their joint acquisition can provide a velocity profile from the surface down to the bedrock contact.

To combine CMP reflection processing and the MASW method, the MASW velocity model was first converted to RMS velocities in time at each CMP location using the Dix formula (Yilmaz 2001). Semblance analysis was then carried out using these velocities before the first reflection. The combined RMS velocity profiles were converted back to interval velocities for the final result.

19.3.4 Interpretation

Results from the MASW survey are shown in Fig. 19.4a. As previously mentioned, due to the very low shear wave velocity in sensitive clay, the MASW method has a limited depth of investigation even if the frequency content of Rayleigh waves is

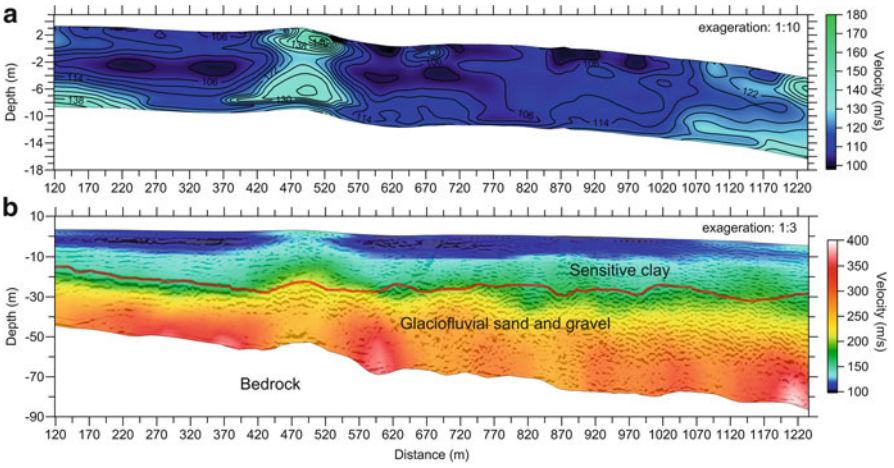

Fig. 19.4 *SV*-wave velocity models obtained from (**a**) MASW alone and (**b**) combined MASW and *SV* reflection processing of the seismic reflection survey. The stacked seismic section overlays the combined velocity profile. Both colormaps are the same but the vertical exaggerations are different due to the large difference in depth for both models

quite low. Because the stratigraphic contacts between the marine unit, the glaciofluvial unit and the bedrock are deep, they cannot be detected using MASW. Moreover, frequencies higher than 15–20 Hz could not be picked for the first mode due to the very high energy content of the higher modes. This limits the resolution of the inversion for depths smaller than 2 m and the accuracy of the velocity layers above 2 m can be questioned. The use of the higher modes in the inversion could solve both of these problems as well as improve the overall accuracy of the velocity model (Xia et al. 2003), especially since very energetic higher modes up to 80 Hz are visible in every dispersion panel for this survey.

Nevertheless, the MASW results are very useful to characterize the variations in shear wave velocity near the ground surface. There is a velocity inversion at a depth of about 4 m due to the contact between the over-consolidated clay layer caused by the freeze thaw cycle and the undisturbed soft clay at depth. The increase in shear wave velocity between depths of 6–12 m is caused by the clay consolidation due to the overburden pressure. Two high velocity anomalies are apparent in the model (Fig. 19.4a): one around 500 m and the other from 1,020 m to the end of the survey line. Both anomalies are likely artefacts associated to topographic variations. No corrections were applied for the topographic variations which are known to affect velocity estimations of MASW (Bodet et al. 2004).

The combined model in Fig. 19.4b extends down to the bedrock contact. As no reflections below the bedrock could be observed, the bedrock velocity cannot be estimated in this survey. This is usually the case in engineering seismology and can be considered a disadvantage compared to seismic refraction survey or MASW. However, the superior depth of investigation and resolution of reflection seismic are major advantages in comparison to the previous methods.

The combined velocity model is overlaid by the *SV* stacked section clipped at depths larger than the bedrock contact. The stacked section greatly improves the geologic interpretation of the velocity model. Two distinct velocity layers can be identified in Fig. 19.4b: (1) the marine unit (90–200 m/s) from the surface down to about 30 m and (2) the glaciofluvial unit (200–400 m/s) at depths larger than 30 m down to the bedrock. The stratigraphic contact between the marine unit and glaciofluvial unit is identified by the orange line. The marine unit shows many parallel reflections which can be interpreted as thin sand beds. The coherency of the glaciofluvial reflections drops after 600 m indicating coarser gravel deposits.

The low velocity anomaly at a distance of about 500 m along the survey line is also apparent at depth in Fig. 19.4b. The topographic variations also affect *SV* reflections and there is no simple solution available to correct these effects. Standard static corrections usually applied to *P*-wave reflections fail for *S*-wave reflections due to the absence of a high impedance contrast near the surface (Yilmaz 2001).

The combined model can be used to assess the seismic hazard parameters of the site. First, this model can give an estimate of VS_{30}. For the velocity model in Fig. 19.4b, the average VS_{30} is 147 m/s, which corresponds to soft clay (Finn and Wightman 2003). The fundamental site resonance period T related to the seismic amplification can also be calculated from the relation $T = 4H/V_{av}$ (Bard and Bouchon 1980) where H is the overburden thickness and V_{av} is the average velocity of the soil. The fundamental site period ranges from 1.19 to 1.89 s for the study site.

19.4 Multi-offset Seismic Piezocone Penetration Test

19.4.1 Data Acquisition and Processing

A multi-offset SCPTu was carried out at a distance of 895 m from the beginning of the survey line (Fig. 19.1) to verify the accuracy of the combined velocity model. The offsets ranged from 1 to 10 m and the receiver depth interval was 1 m. The equipment and the settings used to acquire the data are similar to the ones described in LeBlanc et al. (2006). Two seismic sources were tested: (1) a VIBSIST-20 source based on the swept impact seismic technique (Park et al. 1996) and (2) a 3.6 kg hammer impact on a steel plate lying on the surface of the ground. Only the results with the hammer are presented because they are less affected by noise and their frequency content is similar to the VIBSIST-20 data.

Examples of raw and processed SCPTu shot gathers are given in Fig. 19.5. Two types of noise can be identified in these gathers: ground roll and very high-frequency arrivals. The later is assumed to be sound waves guided by the pushing rods as supported by the high velocity and high frequency of these arrivals. A low-pass filter of 600 Hz was applied to remove this noise. To suppress the ground roll, the signals from the two horizontal accelerometers H1 and H2 embedded in the penetrometer

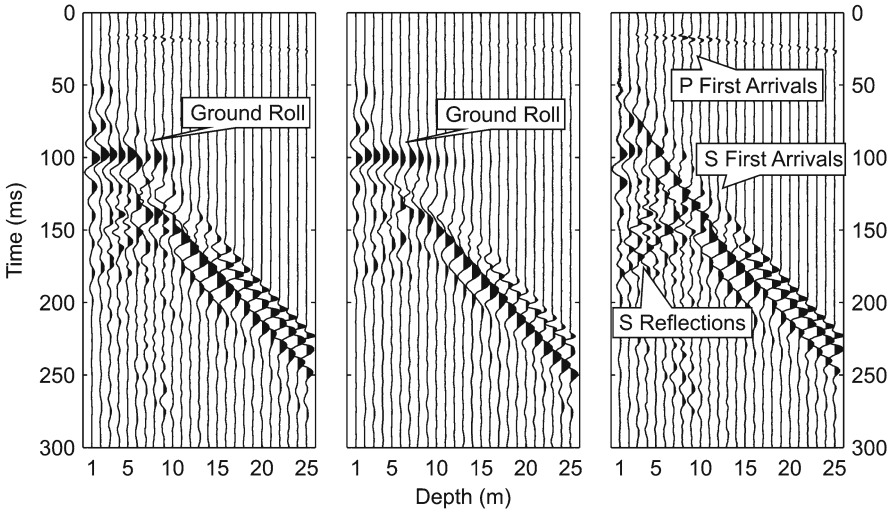

Fig. 19.5 SCPTu shot gathers for a lateral offset of 10 m. The first two gathers are for the two horizontal H1 and H2 accelerometers embedded in the penetrometer. The ground roll noise is completely suppressed in the third gather after the combination of the H1 and H2 gathers

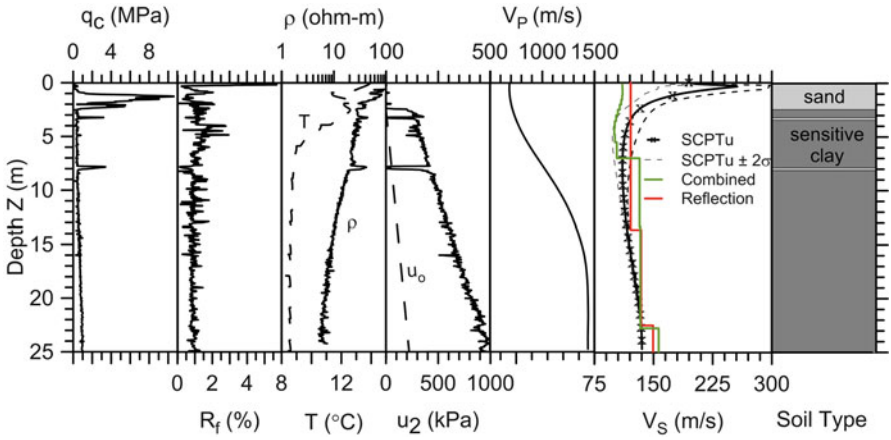

Fig. 19.6 SCPTu logs: cone resistance (q_c), friction ratio (R_f), electrical resistivity (ρ), temperature (T), pore pressure (u_2), *P*- and *S*-waves velocities. The stratigraphic column is interpreted from the SCPTu logs

were combined using the formula $H_{comb} = H_1 - 0.6\ H_2$. The first arrivals were then picked and wavepath eikonal traveltime inversion was carried out using Rayfract (Schuster and Quintus-Bosz 1993). The resulting velocity models were averaged over the length of the multi-offset profile to produce *P*- and *S*-waves vertical seismic profiles (Fig. 19.6).

19.4.2 Interpretation

The piezocone penetration test results were interpreted according to two soil classification charts for ordinary soils, i.e. from Eslami and Fellenius (1997) and from Robertson et al. (1986). The variations of SCPTu parameters as a function of depth and the stratigraphy interpreted from these variations are shown in Fig. 19.6. The two classification charts lead to the same conclusion: a 2 m layer of sand overlays a layer of sensitive clay interbedded with sands. Evidences of sand beds also appear as *S* reflections on the seismic traces and are shown in Fig. 19.5. This confirms the previous interpretation of the seismic reflection profile. The sand and gravel layer below the sensitive clay layer could not be reached due to the limits of the pushing system.

The *S*-wave velocity profiles from the combined method, seismic reflection alone and SCPTu are also compared in Fig. 19.6. The combined and reflection velocity profiles come from the processing of CMP gather no. 151. This CMP is the closest to the SCPTu location. The smooth appearance of the velocity curves for the SCPTu comes from the averaging of the tomographic 2D models not shown herein. This averaging of the multi-offset data improves the accuracy of the 1D velocity profile. To show the dispersion of the data in the 2D model, the velocity profile more or less two times the standard deviation is also plotted in Fig. 19.6.

The three velocity profiles are in good agreement. Using the SCPTu as the reference, the mean absolute errors (MAE) are 15 and 11 % and the root mean square errors (RMSE) are 22 and 19 % for the combined and the reflection profiles respectively. The higher value of the RMSE in both cases is caused by the first 2 m of the models: neither shows the high velocity superficial sand layer. This is to be expected for the reflection model, as it can only give an average velocity for the first few meters. As for MASW, the lack of frequencies higher than 20 Hz for the fundamental mode can explain the misfit above 2 m. Moreover, both measurements were not exactly taken at the same location: the surface survey was carried out on the road shoulder and the SCPTu was acquired in the adjacent orchard, so surface conditions may be different in both locations.

Below 2 m, the MASW and SCPTu models agree very well as the MASW model actually falls inside the standard error limits of the SCPTu. Both models also show the same trend. By removing data above 2 m, RMSE falls at 13 % and MAE at 12 %. This agrees very well with the expected error between MASW and VSP measurements obtained by Xia et al. (2002).

19.5 Discussion and Conclusions

In the case study presented herein, the MASW survey failed to provide the *S*-wave velocity profile from a depth of 12 m down to the bedrock contact. The depth of investigation is so limited that the *S*-wave velocity at 30-m depth Vs_{30} cannot be assessed. Far from being an exceptional case, this is typical for areas with thick

sensitive clay deposits. To avoid this limitation, the combined processing of Rayleigh waves and *SV*-wave reflections is proposed as a solution. Surface waves and *SV*-waves are generated during a typical seismic reflection survey and they can be simultaneously acquired with the proper field parameters. Special care must be taken to avoid aliasing of *SV*-wave reflections by reducing the geophone spacing. To maintain proper spread length, the record of at least 48 live channels with an engineering seismograph is recommended.

Other solutions are available to measure shear wave velocity profiles when the overburden depth exceeds 50 m but they are not as effective as *SV*-wave reflection surveys. Downhole seismic survey is expensive to achieve as the depth becomes too great and seismic information is available at only one location. As for passive MASW surveys, which can go to a depth as great as 100 m, they do not provide as accurate stratigraphy of the soil as reflection seismics. In addition to the velocity assessment, the processing of the *SV*-wave reflections leads to a stacked seismic profile providing the location of stratigraphic contacts along the survey line. Moreover, this can be used to calculate the fundamental site resonance period.

Even in the case of shallow bedrock, *SV*-wave reflections should be considered in MASW records in sensitive clay and their processing would bring better constraints on stratigraphic contacts and add redundancy to velocity estimations. In fact, all seismic arrivals recorded in a typical MASW survey, such as Rayleigh waves, first arrivals, *P*- and *SV*-waves reflections can be processed. In all likelihood, combining the information of these separate techniques gives a far more robust earth model.

Acknowledgments We thank Y. Vincent, S. Bérubé and M. El Baroudi for their help during the acquisition of the geophysical data in the field. We are grateful to Dr. Maarten Vanneste from the NGI for his constructive reviews. The research fund to support this project was provided by the Department of Environment of Québec for the acquisition of data on groundwater in the Outaouais region for the sustainable management of this natural resource.

References

Aylsworth JM, Lawrence DE, Guertin J (2000) Did two massive earthquakes in the Holocene induce widespread landsliding and near-surface deformation in part of the Ottawa Valley, Canada? Geology 28(10):903–906. doi:10.1130/0091-7613(2000)28<903:DTMEIT>2.0.CO;2

Bard PY, Bouchon M (1980) The seismic response of sediment-filled valleys. Part I. The case of incident SH waves. Bull Seismol Soc Am 70:1263–1286

Bélanger JR, Moore A, Prégent A (1997) Surfacial geology, digital map, Thurso Quebec (31G/11). Geological Survey of Canada, Ottawa, Open File Issue 3477

Bodet L, Abraham O, Bitri A, Leparoux D, Côte P (2004) Effect of dipping layers on seismic surface waves profiling: a numerical study. SAGEEP 17:1601. doi:10.4133/1.2923306

Eslami A, Fellenius BH (1997) Pile capacity by direct CPT and CPTu methods applied to 102 case histories. Can Geotech J 34(6):886–904. doi:10.1139/t97-056

Finn WDL, Wightman A (2003) Ground motion amplification factors for the proposed 2005 edition of the National Building Code of Canada. Can J of Civil Eng 30(2):272–278. doi:10.1139/l02-081

LeBlanc AM, Fortier R, Cosma C, Allard M (2006) Tomographic imaging of permafrost using three-component seismic cone penetration test. Geophysics 71(5):H55–H65. doi:10.1190/1.2235876

Margrave GF (2003) Numerical methods of exploration seismology with algorithms in MATLAB. Department of Geology and Geophysics, University of Calgary, Calgary, 225 p

Motazedian DMD, Hunter JHJ (2008) Development of an NEHRP map for the Orleans suburb of Ottawa, Ontario. Can Geotech J 45(8):1180–1188. doi:10.1139/T08-051

Park CB, Miller RM, Steeples DW, Black RA (1996) Swept impact seismic technique (SIST). Geophysics 61(6):1789–1803. doi:10.1190/1.1444095

Park CB, Miller RD, Xia JB (1998) Imaging dispersion curves of surface waves on multi-channel record. SEG Expanded Abs 17(1):1377–1380

Park CB, Miller RD, Miura H (2002) Optimum field parameters of an MASW survey. Exp. Abs SEG-J Tokyo, 17–18 May, pp 22–23

Pugin AJM, Pullan SE, Hunter JA (2009) Multicomponent high-resolution seismic reflection profiling. The Leading Edge 28(10):1248–1261. doi:10.1190/1.3249782

Robertson PK, Campanella RG, Gillespie D, Greig J (1986) Use of piezometer cone data. Use of in situ tests in geotechnical engineering (GSP 6). ASCE, Reston, pp 1263–1280

Schuster GT, Quintus-Bosz A (1993) Wavepath eikonal traveltime inversion: theory. Geophysics 58(9):1314–1323. doi:10.1190/1.1443514

Steeples DW, Miller RD (1998) Avoiding pitfalls in shallow seismic reflection surveys. Geophysics 63(4):1213–1224. doi:10.1190/1.1444422

Xia J, Miller RD, Park CB (1999) Estimation of near-surface shear-wave velocity by inversion of Rayleigh waves. Geophysics 64(3):691–700. doi:10.1190/1.1444578

Xia J, Miller RD, Park CB, Hunter JA, Harris JB and Ivanov J (2002) Comparing shear-wave velocity profiles inverted from multichannel surface wave with borehole measurements. Soil Dyn Earthq Eng 22(3):181–190. http://dx.doi.org/10.1016/S0267-7261(02)00008-8

Xia J, Miller RD, Park CB and Tian G (2003) Inversion of high frequency surface waves with fundamental and higher modes. J Appl Geophys 52(1):45–57. http://dx.doi.org/10.1016/S0926-9851(02)00239-2

Yilmaz Ö (2001) Seismic data analysis: processing, inversion, and interpretation of seismic data, Investigations in geophysics no. 10. SEG Books, Tulsa